

See discussions, stats, and author profiles for this publication at: <https://www.researchgate.net/publication/230577469>

Chiral Conformation at a Molecular Level of a Propeller-Like Open-Shell Molecule on Au(111)

ARTICLE in JOURNAL OF PHYSICAL CHEMISTRY LETTERS · MAY 2012

Impact Factor: 7.46

READS

72

14 AUTHORS, INCLUDING:



M. Pedio

Italian National Research Council

112 PUBLICATIONS 1,301 CITATIONS

SEE PROFILE



Neville V Richardson

University of St Andrews

195 PUBLICATIONS 4,465 CITATIONS

SEE PROFILE



Jean-Pierre Bucher

University of Strasbourg

107 PUBLICATIONS 3,995 CITATIONS

SEE PROFILE



Jaume Veciana

Spanish National Research Council

983 PUBLICATIONS 12,373 CITATIONS

SEE PROFILE

Chiral Conformation at a Molecular Level of a Propeller-Like Open-Shell Molecule on Au(111)

Federico Grillo,^{*,†,§} Veronica Mugnaini,^{‡,‡,§} Malena Oliveros,^{‡,‡} Steve M. Francis,[†] Deung-Jang Choi,[#] Mircea V. Rastei,[#] Laurent Limot,[#] Cinzia Cepek,^{||} Maddalena Pedio,^{||} Stefan T. Bromley,[∇] Neville V. Richardson,[†] Jean-Pierre Bucher,[#] and Jaume Veciana^{*,‡,‡}

[†]EaStCHEM and School of Chemistry, University of St. Andrews, St. Andrews KY16 9ST, United Kingdom

[‡]Institut de Ciència de Materials de Barcelona-CSIC, Campus UAB, E-08193 Bellaterra, Spain

[‡]CIBER de Bioingeniería, Biomateriales y Nanomedicina (CIBER-BBN) Campus Río Ebro - Edificio I+D Bloque 5, 1ª planta c/ Poeta Mariano Esquillor s/n, E-50018 Zaragoza, Spain

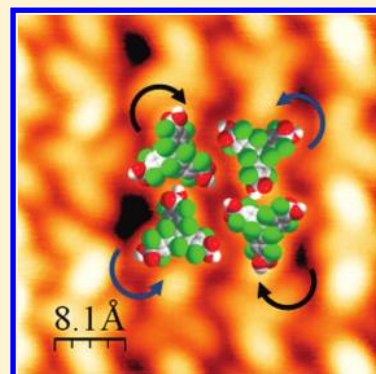
[#]Institut de Physique et Chimie des Matériaux de Strasbourg, UMR 7504, Université de Strasbourg, F-67034 Strasbourg, France

^{||}Istituto Officina dei Materiali del Consiglio Nazionale delle Ricerche, Laboratorio TASC, building MM in AREA Science Park - Basovizza, I-34149 Trieste, Italy

[∇]ICREA (Institució Catalana de Recerca y Estudis Avançats) and Department of Physical Chemistry and Institute of Theoretical and Computational Chemistry (IQTUB), University of Barcelona, E-08028 Barcelona, Spain

Supporting Information

ABSTRACT: A key stage in engineering molecular functional organizations is represented by controlling the supramolecular assembly of single molecular building blocks, tectons, into ordered networks. Here, we show how an open-shell, propeller-like molecule has been deposited under UHV conditions on Au(111) and its supramolecular organization characterized by scanning tunneling microscopy (STM). Racemic islands were observed at room temperature, and their chirality was imaged at the molecular level at low temperature. Modeling further suggests that the observed chirally alternating ordering dominated by intermolecular interactions is energetically favored. Electron paramagnetic resonance and ultraviolet photoemission spectroscopy evidences suggest that the supramolecular networks may preserve the open-shell character of the tecton. These results represent a fundamental step forward toward the engineering of purely organic spintronic devices.



SECTION: Surfaces, Interfaces, Porous Materials, and Catalysis

Control over the supramolecular organization of single molecular building blocks, tectons, into ordered networks on metal surfaces still represents a key stage in the design and engineering of molecular functional organizations.¹ Thus, self-assembled supramolecular structures have been the object of intense investigation over the past decades, and several examples of 2D surface-confined organic² or metal–organic networks have been reported.³ A particularly interesting example of order at the molecular level in such 2D assemblies is displayed in chiral networks,⁴ which have been extensively studied for their potential application in enantioselective catalysis, biosensing, and optoelectronics.^{5–7} In many of those networks, planar carboxylic acids, or their derivatives,⁸ have been the most used tectons, and numerous different 2D orderings have been described. Apart from chirality, several studies have focused on adding different types of functionality to 2D networks, as in the case of metal–organic hybrid architectures, where the unique magnetic properties of the metal ions may be individually addressed, toward the fabrication of spintronic devices,⁹ or paramagnetic organic

molecules. In this latter case, derivatives with a perchlorinated triphenylmethyl skeleton,^{10,11} as well as nitroxide radicals,^{12,13} have been widely investigated and used to transfer paramagnetism to solid supports, engineering novel molecular devices that are highly promising for their potential use as robust spintronic devices because they have been shown to retain their open-shell character when adsorbed in an up-right configuration.

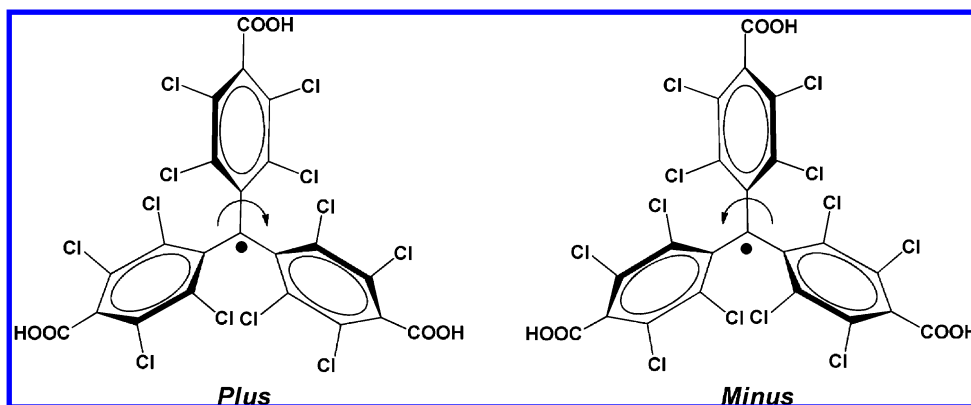
In this Letter, we report on a significant advance toward the fabrication under ultra high vacuum (UHV) conditions of functional, purely organic, racemic 2D networks formed by an unusual chiral and paramagnetic tecton, the tris-*p*-carboxylic-polychlorotriphenylmethyl radical acid derivative (PTMTC, Scheme 1),^{14,15} whose three para carboxylic groups can drive

Received: March 31, 2012

Accepted: May 22, 2012

Published: May 22, 2012

Scheme 1. Chemical Structure of the Tris-*p*-carboxylicpolychlorotriphenylmethyl Radical Acid in Its Two Enantiomeric Forms, Plus and Minus



the formation of hydrogen-bonded networks in the solid state.¹⁴

The steric hindrance of the three pairs of chlorine atoms in the ortho positions with respect to the central carbon atom is responsible for the concerted torsion of the three phenyl rings along the $C_{\text{central}}-C_{\text{bridgedhead}}$ bonds with a resulting propeller-like conformation. This generates two enantiomeric atropoisomeric conformations, one in which the three phenyl rings are clockwise rotated (Plus) and the other in which the rotation is counterclockwise (Minus)¹⁰ when viewed from the central carbon atom. Moreover, the central sp^2 carbon atom formally carries an unpaired electron whose reactivity is suppressed by the steric protection produced by the three pairs of *ortho*-chlorine atoms; these also confer to the radical an unprecedented persistency, as well as high thermal and chemical stability, that suggested the feasibility of its sublimation under appropriate UHV conditions. X-ray photoemission (XP) spectra of monolayer and multilayer preparations were recorded (see Supporting Information, Figure S11). The collected data confirmed that the PTMTC molecule could be successfully sublimed in vacuum and dosed onto the surface, being all the expected Cl, C, and O chemical species present. Because it is well-known that the PTMTC radical is a good electron-acceptor species that may generate, by an electron transfer under soft conditions, the corresponding negatively charged species, that is, the anion¹⁰ one, it was considered important to investigate whether the open-shell electronic configuration of the PTMTC molecules could be maintained. By recording the electron paramagnetic resonance (EPR) spectrum of a PTMTC multilayer, obtained by sublimation under UHV conditions on Au/mica and then brought to air, an asymmetric EPR signal at a g value of 2.0023, typical for an immobilized PTM radical derivative in the solid state (see Figure S12, Supporting Information),^{11a} was detected, thus suggesting that the physisorbed multilayer was still paramagnetic, much like the bulk compound. In addition, to gain insight also into the electronic configuration of the molecules directly in contact with the Au(111) surface, ultraviolet photoemission spectroscopy (UPS) was used (see section S13, Supporting Information). Figure 1 shows the UP spectra recorded for a multilayer coverage, prepared as for the EPR experiments, for the monolayer one and their comparison with the emission spectrum of the clean Au(111).

On the spectrum of the multilayer sample, molecular adsorption produces broad features. Of these, the one corresponding to the first occupied molecular state (at ~ 1.6

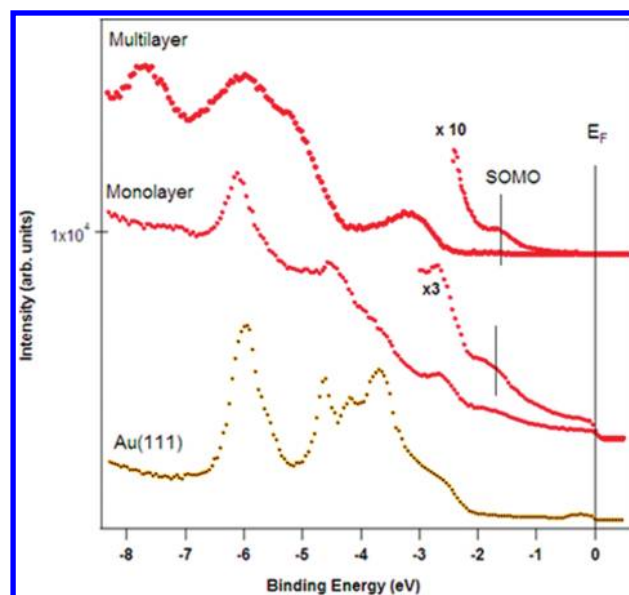


Figure 1. Ultraviolet valence-band photoemission spectra for multilayer, in dark red, (~ 20 molecular layers; see section S13, Supporting Information), and monolayer, in red, PTMTC adsorptions on the Au(111) surface and clean Au(111), in orange. The peak at ~ 1.6 eV is assigned to the SOMO molecular state.

eV) and detectable in a region of flat emission for the clean sample may be attributed to the single occupied molecular orbital (SOMO) of the molecule.^{16,17} The presence of this feature also in the monolayer spectrum suggests that the molecule may not change its open-shell electronic configuration when physisorbed on the gold surface. Nevertheless, further experiments are in progress to clarify the details of the interaction occurring at the interface. Using the vibrational-spectroscopy-based techniques, reflection absorption infrared spectroscopy (RAIRS) and high-resolution electron energy loss spectroscopy (HREELS) on PTMTC/Au(111), it has been possible to gain information also on the intermolecular interactions between the adsorbed molecules, their orientation with respect to the surface (see Figure S13, Supporting Information), as well as the thermal stability of the prepared layers. In particular, the position of the band corresponding to the carbonyl vibrations (~ 1725 cm^{-1} , Figure S13a, Supporting Information), intermediate between the value for the isolated molecule as determined by DFT calculations (~ 1790 cm^{-1}) and that in the solid state (~ 1670 cm^{-1}), suggests a limited

degree of intermolecular H-bonding interactions involving the carboxylic acid groups when PTMTC is adsorbed onto the Au(111) surface. The band at $\sim 870\text{ cm}^{-1}$ is assigned to the C–Cl stretch.¹⁸ This value, on the higher side of the energy range expected for this mode, suggests that also some of the C–Cl groups are involved in intermolecular interactions, as will be described later. HREELS measurements (Figure SI3b–f, Supporting Information) indicate an increased degree of ordering after annealing to $\sim 325\text{--}350\text{ K}$. Desorption of loosely bound species and the onset of the C–Cl bond cleavage occur between 350 and 400 K. Extensive deterioration of the adlayer is seen at above 450 K. Room-temperature STM images of submonolayer preparations, obtained after annealing to $\sim 350\text{ K}$, show the formation of molecular islands (Figure 2A), with a well-defined internal structure surrounded by disordered areas.

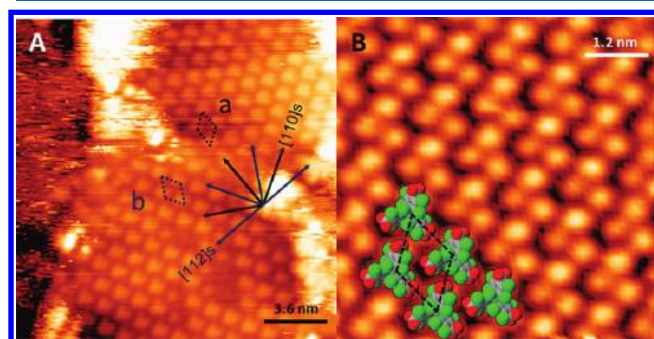


Figure 2. Room-temperature STM topographic images of a submonolayer PTMTC radical on Au(111). Image A shows an island in which the unit cells of domains *a* and *b* are rotated by 30° with respect to each other. Some defects characterized by a (2×2) periodicity are observed in domain *b*. These are thought to represent chlorine atoms adsorbed on gold.¹⁹ Image B shows increased resolution on domain *a* to which molecular models have been added for clarity. The model is shown as homochiral for simplicity. The dashed line represents the unit cell. (A) $18 \times 18\text{ nm}^2$; (B) $6 \times 6\text{ nm}^2$; (-1.3 V , 0.2 nA).

The islands show a hexagonal molecular arrangement, corresponding to (4×4) and $(4 \times 4)R30^\circ$ superstructures, the latter one being incommensurate, with a density of ~ 0.9 molecules per nm^2 , which is different from that observed within the layers of molecules in single crystals of PTMTC.¹⁴ This

suggests that, in the absence of interlayer molecular–molecular interactions, as occurs in bulk crystals, an alternative 2D ordering of PTMTC molecules is energetically preferred on a gold surface. In the two islands shown in Figure 2A, where each bright spot corresponds in size to one single molecule, the intermolecular distance is $\sim 1.13\text{ nm}$, consistent with the formation of a supramolecular assembly. It is worth noting that, unusually for a three-fold symmetric surface, molecular domain *a* (Figure 2A) is aligned along close-packed directions, while the second domain, *b*, is rotated by 30° with respect to it. The alternative domain orientations indicate that the gold surface is a minor perturbation on the intermolecular interactions within the layer, although it is sufficient to impose an alignment with either the $[1\bar{1}0]$ or the $[11\bar{2}]$ substrate directions. Higher-resolution images of domain *a* (Figure 2B) show that each PTMTC molecule appears as a set of three bright, although unequal, maxima, each having a diameter of $\sim 0.6\text{ nm}$ corresponding to a substituted phenyl ring. A model of this 2D surface-confined layer, highlighting some of the intermolecular interactions thought to occur, is reported in Figure SI4 (Supporting Information), together with the comparison with a calculated STM image (Figure SI5, Supporting Information), which qualitatively reproduces the different contrast of each of the lobes in Figure 2B. This is thought to be an effect of the lateral variation in the van der Waals (vdW) interactions between the surface and the phenyl rings within a molecule. The intermolecular packing is thought to derive from a subtle balance between repulsive $\text{Cl}\cdots\text{Cl}$ interactions and attractive $\text{Cl}\cdots\text{HO}$ weak H-bonding intermolecular interactions, reported to play an important role in molecular self-assembly.²⁰ A second supramolecular organization was observed at room temperature but could not be easily imaged; therefore, low-temperature STM measurements were performed in order to resolve it in more detail. The topographic images obtained at 4.6 K (Figure 3, more details are given in section SI6, Supporting Information) resolved a $\sim 20\%$ more densely packed assembly based on a four-molecule elementary unit, rhombic and incommensurate, $\sim (2 \times 1.8)\text{ nm}^2$ in size.

The apparent absence of hexagonal domains at low temperature may suggest that such structures may be stable only at room or higher temperatures. The enhanced resolution available at lower temperature allowed additional submolecular features to be imaged, particularly at lower bias voltages. Each

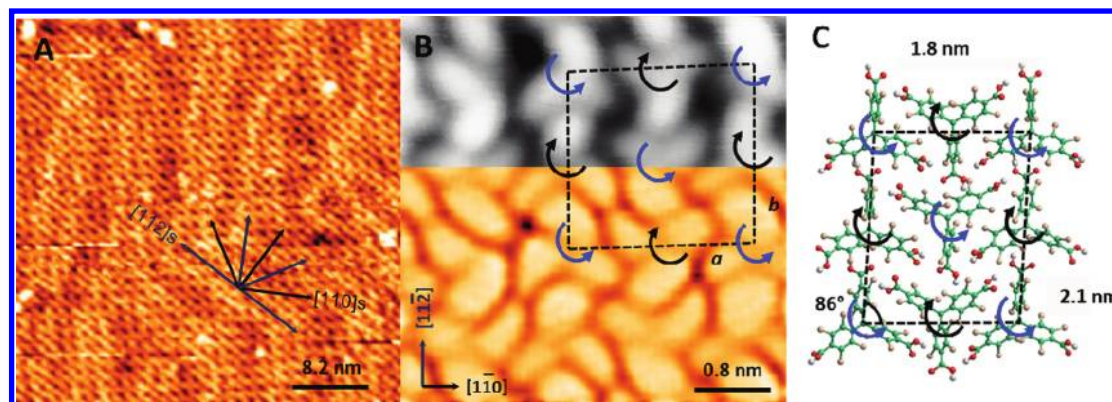


Figure 3. (A) STM topography of a PTMTC radical adsorbed on Au(111) obtained at 4.6 K ($41 \times 41\text{ nm}^2$, -3.2 V , 30 pA). (B) Combined STM topographic (gray scale) and Laplacian filtered (color scale) image ($4 \times 4\text{ nm}^2$, -3.2 V , 30 pA). Unit cell (dashed line) vectors are $a = 2.0 \pm 0.05\text{ nm}$ and $b = 1.8 \pm 0.05\text{ nm}$; curly arrows indicate the chirality of each molecule: Minus enantiomer, blue arrows, and Plus enantiomer, black arrows. (C) A nine-molecule (3×3) cluster model obtained by energy minimization using the GAFF force field.

lobe of any individual PTMTC molecule could be imaged, and the contrast variation of the lobes in the STM image (Figure 3B, top) suggests that, as described for the room-temperature STM images, the strength of the interaction with the surface is likely to be different for each of the three lobes of each molecule, implying that the phenyl rings have notably different interactions with the gold surface. In addition, the chiral propeller-like conformation of each molecule could be imaged, showing the formation of racemic domains. Figure 3B shows that, along the $[1-10]$ direction, Minus (represented by the blue arrows) and Plus (black arrows) molecules are oriented alternately up and down. Along the $[11-2]$ direction, Plus and Minus molecules still alternate, but within the same row, they all point either up or down. As suggested also by the room-temperature STM images, the PTMTC interaction with the Au(111) surface is likely to be determined by numerous weak Cl–Au vdW interactions, the sum of which is responsible for the thermal stability of the observed domains. Classical force field modeling was employed to energy minimize the H-bonded 2D rhombic-ordered assemblies of PTMTC molecules at low temperature. The generalized AMBER force field (GAFF²¹ as implemented in the Hyperchem²² program) and (2×2) and (3×3) molecule 2D assemblies in the absence of the gold substrate were used. At least as a good first approximation, the modeling of the PTMTC on the Au(111) system by the corresponding gas-phase 2D molecular assembly is justified on the basis of recent, high-level electronic structure calculations that have confirmed that molecule–Au(111) interactions insignificantly affect the intermolecular H-bonding²³ or the lateral variation of the vdW interactions,²⁴ which instead mainly determine the difference in energetic stability of possible competing 2D molecular arrangements. The modeling shows that PTMTC molecule arrangements, which had some degree of nearest-neighbor alternation of chirality, were always among the most energetically favored orderings. Specifically, all models having some chiral alternation were found to lie in a narrow band of energies (width ≈ 5 kJ/mol per PTMTC molecule), with the lowest-energy model not having any chiral alternation being at least 12 kJ/mol per PTMTC molecule higher in energy. Interestingly, one of the lowest-energy models (Figure 3C) exhibits the maximum possible chiral alternation (i.e., a change of chirality every nearest neighbor) and reproduces the supramolecular assembly observed in low-temperature STM reasonably well. The dimensions of the (3×3) model in Figure 3C $[(1.8 \times 2.1) \text{ nm}^2]$ match reasonably fine with the unit cell highlighted in Figure 3B, with the discrepancies likely due to the neglect of the gold surface. The reasonable correspondence between modeling and experiment further confirms that the observed ordering is chirally alternating and dominated by intermolecular H-bonding.

In conclusion, by UHV sublimation, we deposited an open-shell molecule, the PTMTC radical, on Au(111), and using STM, we imaged the surface-confined 2D assemblies of such a nonplanar derivative at room and at low temperature. In both cases, the supramolecular, self-assembled structures were aligned with the high-symmetry directions of the Au(111) substrate and were different from those characteristic of the bulk crystals. Low-temperature STM allowed the chirality of each molecule to be imaged and the assemblies to be identified as racemic. EPR and preliminary UPS investigation suggest that the electronic open-shell configuration might be retained upon UHV sublimation and deposition on Au(111). These results

represent a fundamental step toward the engineering of purely organic spintronic devices.

■ EXPERIMENTAL SECTION

Preparation Procedure. The Au(111) single-crystal surfaces were cleaned in situ by standard Ar⁺ sputtering and annealing procedures. The PTMTC was dosed by vacuum sublimation at a dosing temperature of ~ 435 K onto a Au(111)-(22 \times $\sqrt{3}$) reconstructed surface held at room temperature. Doser calibration was initially determined via a quartz crystal microbalance and optimized via XPS.

UPS. Ultraviolet VB photoemission spectra were acquired in a UHV chamber with a base pressure of 3×10^{-10} mbar using a conventional He discharge lamp ($h\nu = 21.2$ eV). Electron-energy distribution curves were measured at normal incidence with an overall instrumental energy resolution of 0.120 eV. Binding energy values are referred to the Fermi level of the clean gold crystal.

STM. STM measurements were performed in two independent UHV systems; these include RT measurements (VT-STM, Omicron, base pressure below 5×10^{-10} mbar) and low-temperature (LT) measurements (LT-STM, Omicron, base pressure below 5×10^{-11} mbar). For LT measurements, PTMTC was dosed as described above and then immediately transferred to the LT-STM, which had been previously cooled to 4.6 K. Electrochemically etched tungsten tips, cleaned in situ by ion bombardment and flash annealing, were used. Images were analyzed using the WSxM software package.²⁵

■ ASSOCIATED CONTENT

§ Supporting Information

XP spectra, multilayer EPR spectrum, vibrational spectroscopy (RAIR, HREEL), further modeling, and additional LT-STM images. This material is available free of charge via the Internet at <http://pubs.acs.org>.

■ AUTHOR INFORMATION

Corresponding Author

*E-mail: federico.grillo@st-andrews.ac.uk. Fax: +44 (0) 1334 46 3808 (F.G.); E-mail: vecianaj@icmab.es. Fax: +34 93 580 5729 (J.V.).

Author Contributions

[§]These authors contributed equally to this work.

Notes

The authors declare no competing financial interest.

■ ACKNOWLEDGMENTS

The authors thank the European Union for financing the SURMOF project (NMP4-CT-2006-032109), the ANR, France, for financing the SPINMASTER project, and the Spanish MICINN for financing the POMAs (CTQ2010-19501/BQU) and FIS2008-02238 projects. St Andrews team acknowledges the EaStCHEM Research Computing Facility and H. Früchtl for computational support. V.M. acknowledges the MICINN for a Juan de la Cierva postdoctoral grant. V.M., M.O., and J.V. acknowledge CIBER-BBN, an initiative funded by the VI National R&D&i Plan 2008-2011, Iniciativa Ingenio 2010, Consolider Program, CIBER Actions and financed by the Instituto de Salud Carlos III with assistance from the European Regional Development Fund. The Strasbourg team acknowledges support from the International Center for Frontier Research in Chemistry.

DEDICATION

Dedicated to Prof. Concepció Rovira on the occasion of her birthday.

REFERENCES

- (1) (a) Lehn, J. M. *Supramolecular Chemistry: Concepts and Perspectives*; VCH: Weinheim, Germany, 1995. (b) Jones, W., Rao, C. N. R., Eds; *Supramolecular Organizations and Materials Design*; Cambridge University Press: New York, 2002. (c) Ozin, G.; Arsenault, A. *Nanochemistry: A Chemical Approach to Nanomaterials*; Royal Society of Chemistry: Cambridge, U.K., 2005.
- (2) (a) Barth, J. V.; Costantini, G.; Kern, K. Engineering Atomic and Molecular Nanostructures at Surfaces. *Nature* **2005**, *437*, 671–679. (b) Schreiber, F. Structure and Growth of Self-Assembling Monolayers. *Prog. Surf. Sci.* **2000**, *65*, 151–256. (c) Rosei, F.; Schunack, M.; Naitoh, Y.; Jiang, P.; Gourdon, A.; Laegsgaard, E.; Stensgaard, I.; Joachim, C.; Besenbacher, F. Properties of Large Organic Molecules on Metal Surfaces. *Prog. Surf. Sci.* **2003**, *71*, 95–146. (d) Barth, J. V.; Weckesser, J.; Cai, C.; Günter, P.; Bürgi, L.; Jeandupeux, O.; Kern, K. Building Supramolecular Nanostructures at Surfaces by Hydrogen Bonding. *Angew. Chem., Int. Ed.* **2000**, *39*, 1230–1234. (e) Payer, D.; Comiso, A.; Dmitriev, A.; Strunskus, T.; Lin, N.; Wöll, Ch.; De Vita, A.; Barth, J. V.; Kern, K. Ionic Hydrogen Bonds Controlling Two-Dimensional Supramolecular Systems at a Metal Surface. *Chem.—Eur. J.* **2007**, *13*, 3900–3906. (f) Cañas-Ventura, M. E.; Xiao, W.; Wasserfallen, D.; Müllen, K.; Brune, H.; Barth, J. V.; Fasel, R. Self-Assembly of Periodic Bicomponent Wires and Ribbons. *Angew. Chem., Int. Ed.* **2007**, *46*, 1814–1818.
- (3) (a) Lin, N.; Stepanow, S.; Ruben, M.; Barth, J. V. Surface-Confining Supramolecular Coordination Chemistry. In *Topics in Current Chemistry*; Springer-Verlag: Berlin, Heidelberg, Germany, 2009; Vol. 287, pp 1–44. (b) Björk, J.; Matena, M.; Dyer, M. S.; Enache, M.; Lobo-Checa, J.; Gade, L. H.; Jung, T. A.; Stöhr, M.; Persson, M. STM Fingerprint of Molecule–Atom Interactions in a Self-Assembled Metal–Organic Surface Coordination Network on Cu(111). *Phys. Chem. Chem. Phys.* **2010**, *12*, 8815–8821.
- (4) (a) Dmitriev, A.; Spillmann, H.; Stepanow, S.; Strunskus, T.; Wöll, Ch.; Seitsonen, A. P.; Lingenfelder, M.; Lin, N.; Barth, J. V.; Kern, K. Asymmetry Induction by Cooperative Intermolecular Hydrogen Bonds in Surface-Anchored Layers of Achiral Molecules. *ChemPhysChem* **2006**, *7*, 2197–2204. (b) Schoeck, M.; Otero, R.; Stojkovic, S.; Huemmelink, F.; Gourdon, A.; Laegsgaard, E.; Stensgaard, I.; Joachim, C.; Besenbacher, F. Asymmetry Induction by Cooperative Intermolecular Hydrogen Bonds in Surface-Anchored Layers of Achiral Molecules. *J. Phys. Chem. B* **2006**, *110*, 12835–12838.
- (5) (a) Mark, A. G.; Forster, M.; Raval, R. Direct Visualization of Chirality in Two Dimensions. *Tetrahedron: Asymmetry* **2010**, *21*, 1125–1134. (b) McFadden, C. F.; Cremer, P. S.; Gellman, A. J. Adsorption of Chiral Alcohols on “Chiral” Metal Surfaces. *Langmuir* **1996**, *12*, 2483–2487. (c) Izumi, Y. Modified Raney Nickel (MRNi) Catalyst: Heterogeneous Enantio-Differentiating (Asymmetric) Catalyst. *Adv. Catal.* **1983**, *32*, 215–271. (d) Johannes, H. X.; Elemans, A. A. W.; De Cat, I.; De Feyter, S. Two-Dimensional Chirality at Liquid–Solid Interfaces. *Chem. Soc. Rev.* **2009**, *38*, 722–736. (e) Rosi, N. L.; Mirkin, C. Nanostructures in Biodiagnostics. *Chem. Rev.* **2005**, *105*, 1547–1562. (f) Schiffrin, A.; Riemann, A.; Auwärter, W.; Pennec, Y.; Weber-Bargioni, A.; Cvetko, D.; Cossaro, A.; Morgante, A.; Barth, J. V. Zwitterionic Self-Assembly of L-Methionine Nanogratings on the Ag(111) Surface. *Proc. Natl. Acad. Sci. U.S.A.* **2007**, *104*, 5279–5284.
- (6) Ernst, K.-H. Supramolecular Surface Chirality. In *Topics in Current Chemistry*; Springer-Verlag: Berlin, Heidelberg, Germany, 2006; Vol. 265, pp 209–252.
- (7) (a) Classen, T.; Lingenfelder, M.; Wang, Y.; Chopra, R.; Virojanadara, C.; Starke, U.; Costantini, G.; Fratesi, G.; Fabris, S.; de Gironcoli, S.; et al. Hydrogen and Coordination Bonding Supramolecular Structures of Trimesic Acid on Cu(110). *J. Phys. Chem. A* **2007**, *111*, 12589–12603. (b) Zhang, J.; Li, B.; Cui, X.; Wang, B.; Yang, J.; Hou, J. G. Spontaneous Chiral Resolution in Supramolecular Assembly of 2,4,6-Tris(2-pyridyl)-1,3,5-triazine on Au(111). *J. Am. Chem. Soc.* **2009**, *131*, 5885–5890. (c) Chen, Q.; Frankel, D. J.; Richardson, N. V. Self-Assembly of Adenine on Cu(110) Surfaces. *Langmuir* **2002**, *18*, 3219–3225.
- (8) (a) Dmitriev, A.; Lin, N.; Weckesser, J.; Barth, J. V.; Kern, K. Supramolecular Assemblies of Trimesic Acid on a Cu(100) Surface. *J. Phys. Chem. B* **2002**, *106*, 6907–6912. (b) Frederick, B. G.; Leible, F. M.; Haq, S.; Richardson, N. V. Evolution of Lateral Order and Molecular Reorientation in the Benzoate/Cu(110) System. *Surf. Rev. Lett.* **1996**, *3*, 1523–1546.
- (9) (a) Ruben, M.; Rojo, J.; Romero-Salguero, F. J.; Uppadine, L. H.; Lehn, J.-M. Grid-Type Metal Ion Architectures: Functional Metallosupramolecular Arrays. *Angew. Chem., Int. Ed.* **2004**, *43*, 3644. (b) Gambardella, P.; Stepanow, S.; Dmitriev, A.; Honolka, J.; de Groot, F. M. F.; Lingenfelder, M.; Gupta, S. S.; Sarma, D. D.; Bencock, P.; Stancu, S.; et al. Supramolecular Control of the Magnetic Anisotropy in Two-Dimensional High-Spin Fe Arrays at a Metal Interface. *Nat. Mater.* **2009**, *8*, 189–193. (c) Carbone, C.; Gardonio, S.; Moras, P.; Lounis, S.; Heide, M.; Bihlmayer, G.; Atodiresi, N.; Dederichs, P. H.; Blugel, S.; Vlaic, S.; et al. Self-Assembled Nanometer-Scale Magnetic Networks on Surfaces: Fundamental Interactions and Functional Properties. *Adv. Funct. Mater.* **2011**, *21*, 1212–1228.
- (10) Veciana, J.; Ratera, I. Polychlorotriphenylmethyl Radicals: Towards Multifunctional Molecular Materials. In *Stable Radicals: Fundamentals and Applied Aspects of Odd-Electron Compounds*; Hicks, R. G., Ed.; Wiley: New York, 2010; pp 33–80.
- (11) (a) Mas-Torrent, M.; Crivillers, N.; Mugnaini, V.; Ratera, I.; Rovira, C.; Veciana, J. Organic Radicals on Surfaces: Towards Molecular Spintronics. *J. Mater. Chem.* **2009**, *19*, 1691–1695. (b) Simão, C.; Mas-Torrent, M.; Crivillers, N.; Lloveras, V.; Artes, J. M.; Gorostiza, P.; Veciana, J.; Rovira, C. A Robust Molecular Platform for Non-Volatile Memory Devices with Optical and Magnetic Responses. *Nat. Chem.* **2011**, *3*, 359–364. (c) Crivillers, N.; Furukawa, S.; Minoia, A.; Ver Heyen, A.; Mas-Torrent, M.; Sporer, C.; Linares, M.; Volodin, A.; Van Haesendonck, C.; Van der Auweraer, M.; et al. Two-Leg Molecular Ladders Formed by Hierarchical Self-Assembly of an Organic Radical. *J. Am. Chem. Soc.* **2009**, *131*, 6246–6252.
- (12) Robin, A.; Marnell, L.; Bjork, J.; Dyer, M. S.; Silva Bermudez, P.; Haq, S.; Barrett, S. D.; Persson, M.; Minoia, A.; Lazzaroni, R.; et al. Adsorption and Organization of the Organic Radical 3-Carboxyproxyl on a Cu(110) Surface: A Combined STM, RAIRS, and DFT Study. *J. Phys. Chem. C* **2009**, *113*, 13223–13230.
- (13) Mannini, M.; Sorace, L.; Gorini, L.; Piras, F. M.; Caneschi, A.; Magnani, A.; Menichetti, S.; Gatteschi, D. Self-Assembled Organic Radicals on Au(111) Surfaces: A Combined ToF-SIMS, STM, and ESR Study. *Langmuir* **2007**, *23*, 2389–2397.
- (14) MasPOCH, D.; Domingo, N.; Ruiz-Molina, D.; Wurst, K.; Vaughan, G.; Tejada, J.; Rovira, C.; Veciana, J. A Robust Purely Organic Nanoporous Magnet. *Angew. Chem., Int. Ed.* **2004**, *43*, 1828–1832.
- (15) The two enantiomers are named Plus and Minus according to the accepted CIP nomenclature; see: Cahn, R. S.; Ingold, C.; Prelog, V. Specification of Molecular Chirality. *Angew. Chem., Int. Ed.* **1966**, *5*, 385–415.
- (16) Crivillers, N.; Munuera, C.; Mas-Torrent, M.; Simão, C.; Bromley, S. T.; Ocal, C.; Rovira, C.; Veciana, J. Dramatic Influence of the Electronic Structure on the Conductivity through Open- and Closed-Shell Molecules. *Adv. Mater.* **2009**, *21*, 1177–1181.
- (17) Crivillers, N.; Paradinas, M.; Mas-Torrent, M.; Bromley, S. T.; Rovira, C.; Ocal, C.; Veciana, J. Negative Differential Resistance (NDR) in Similar Molecules with Distinct Redox Behavior. *Chem. Commun.* **2011**, *47*, 4664–4666.
- (18) Shekhar, O.; Roques, N.; Mugnaini, V.; Munuera, C.; Ocal, C.; Veciana, J.; Wöll, Ch. Grafting of Monocarboxylic Substituted Polychlorotriphenylmethyl Radicals onto a COOH-Functionalized Self-Assembled Monolayer through Copper (II) Metal Ions. *Langmuir* **2008**, *24*, 6640–6648.

(19) Gao, W.; Baker, T. A.; Zhou, L.; Pinnaduwa, D. S.; Kaxiras, E.; Friend, C. M. Chlorine Adsorption on Au(111): Chlorine Overlay or Surface Chloride? *J. Am. Chem. Soc.* **2008**, *130*, 3560–3565.

(20) (a) Hathwar, V. R.; Guru Row, T. N. Nature of Cl...Cl Intermolecular Interactions via Experimental and Theoretical Charge Density Analysis: Correlation of Polar Flattening Effects with Geometry. *J. Phys. Chem. A* **2010**, *114*, 13434–13441. (b) Cohen, M. D.; Elgavi, A.; Green, B. S.; Ludmer, Z.; Schmidt, G. M. J. Photodimerization and Excimer Emission in a Crystalline 1,4-Diphenylbutadiene. *J. Am. Chem. Soc.* **1972**, *94*, 6776–6779. (c) Sarma, J. A. R. P.; Desiraju, G. R. The Role of Cl...Cl and C–H...O Interactions in the Crystal Engineering of 4-Å Short-Axis Structures. *Acc. Chem. Res.* **1986**, *19*, 222–228. (d) Ramamutry, V.; Venkatesan, K. Photochemical Reactions of Organic Crystals. *Chem. Rev.* **1987**, *87*, 433–481.

(21) Weiner, S. J.; Kollman, P. A.; Case, D. A.; Singh, U. C.; Ghio, C.; Alagona, G.; Profeta, S., Jr.; Weiner, P. A New Force Field for Molecular Mechanical Simulation of Nucleic Acids and Proteins. *J. Am. Chem. Soc.* **1984**, *106*, 765–784.

(22) *HyperChem(TM) Professional 7.51*; Hypercube, Inc.: Gainesville, FL.

(23) Mura, M.; Gulans, A.; Thonhauser, T.; Kantorovich, L. Role of van der Waals Interaction in Forming Molecule–Metal Junctions: Flat Organic Molecules on the Au(111) Surface. *Phys. Chem. Chem. Phys.* **2010**, *12*, 4759–4767.

(24) Nguyen, M.-T.; Pignedoli, C. A.; Treier, M.; Fasel, R.; Passerone, D. The Role of van der Waals Interactions in Surface-Supported Supramolecular Networks. *Phys. Chem. Chem. Phys.* **2010**, *12*, 992–999.

(25) Horcas, I.; Fernandez, R.; Gomez-Rodriguez, J. M.; Colchero, J.; Gomez-Herrero, J.; Baro, A. M. WSXM: A Software for Scanning Probe Microscopy and a Tool for Nanotechnology. *Rev. Sci. Instrum.* **2007**, *78*, 013705.